GEOMATH

FINAL REPORT

BN-Energy Company Ltd.

Application of Euler Deconvolution and Analytical Signal Derivatives for Structural Interpretation of Satellite Gravity related to Gold Mineralization Zones

Block RS-12V

West Portsudan, Red Sea State

PD., PhD., M.Sc., B.Sc. Dr. Khalid Mustafa Kheiralla
khalidkheiralla@gmail.com

23/10/2025

Contents

Application of Euler Deconvolution and Analytical Signal Derivatives for Structural Interpretation of Satellite Gravity related to Gold Mineralization Zones

1. INTRODUCTION

BM Energy mining Project lies in the western part of Portsudan in the Red Sea State. The rocks of the Proterozoic era Basement Complex characterize the area. On the other hand, the area is located in the Arabian Nubian shield (ANS), which is of great importance to Sudan in terms of and mineral wealth.

This report represents the preliminary findings of the regional geological assessment on the BM Energy mining concession area. On the other hand, geophysical investigation in the form of Satellite Gravity carried out to locate mineralization zones in BM Energy block RS 12V.

This report presents the theoretical background and computational workflow for gravity data correction and enhancement used in geophysical exploration. The methods include Free-Air and Bouguer corrections, calculation of Complete Bouguer Anomaly (CBA), regional–residual separation, vertical derivatives, analytical signal, horizontal gradient, and Euler Deconvolution for depth estimation and source geometry interpretation.

2. SURVEY DETAILS

The project is located in Red Sea State, west Portsudan and cover by Portsudan topographic sheet. The project area is mapped as shown in Figure (1) and defined by the following coordinates in Table (1). All data grids, ArcMap images and maps are provided in the following projection:

Table 1. coordinates of Block RS 12V

Longitude			Latitude			East (X)	North (Y)	corner	Area(km²)
36	51	36.6	19	45	40	275786.03	2186462.25	A	264
36	57	21.6	19	45	40	285830.94	2186338.19	B	Zone 37Q
36	57	21.6	19	31	26.4	285516.00	2160087.51	C	
36	51	36.6	19	31	26.4	275456.30	2160210.31	D	

BN ENERGY concession area comprises an exclusive Exploration License granted by the Ministry of Minerals for BN ENERGY MINING CO. The total area is around 265 km^2, and lies 30 km west of Portsudan town on the Red Sea State.

BN ENERGY concession area is a rectangular block with its major axis north south. It is a rugged desert terrain with wadis with extensive flood plains form fans surrounding the massifs. Several wadis are the main drainage system, runs from east to west, and roughly, with its tributaries, dissects the whole blocks. Flow is dependent on the seasonal but occasional monsoons during December-March. Red Sea State lies within the dry desert regime. Rain is scarce (<200mm), which manifests the rare vegetation and mostly along wadis. Within such an understanding, it is anticipated the intended activities and operations would have some environmental and social impacts on the environment of the area.

Fig. 1. Location of study area

The survey was planned to provide regional geophysical investigation for gold and Gold Ore Deposits, Satellite Gravity and airborne magnetic data coverage over block RS 12V, totaling 264 km^2.

3. GEOLOGICAL SETTING

The concession Block RS-12V and occupies an area of about 264 km^2 located in the northern part of the Late Proterozoic Pan-African Nubian Shield of NE Sudan which is comprised of juvenile volcano-sedimentary sequences of oceanic island arcs affinities. The area has not been mapped in detailed before. In the present work ETM+ images interpretation of rock units together with the available information has been used to produce the geological map of the area (Fig. 2).

The litho-stratigraphic Sequence for the rock Units According to the earlier previous work, the oldest sequence in the area around Block RS-12V is meta-volcano-sedimentary sequence. This sequence was subjected to folding, faulting and green-schist facies of regional metamorphism, Subsequently the sequence was intruded by syn-orogenic granitoids occupying large areas and traversed by frequent dyke swarms. The most recent event in the area is the emplacement of Late to Post orogenic complexes which were in turn followed by the injection of further dyke swarms.

The Unconsolidated recent sediments cover some areas in the Block. Unconsolidated Sediments Dykes and Veins Late tectonic granitic complex Syn- Orogenic Granitoids Ophiolitic Mafic-Ultramafic Complexes Low grade Metavolcano-sedimentary Sequence.

Geological base maps at scale of 1:100000 have been constructed for the concession area (Fig. 2).

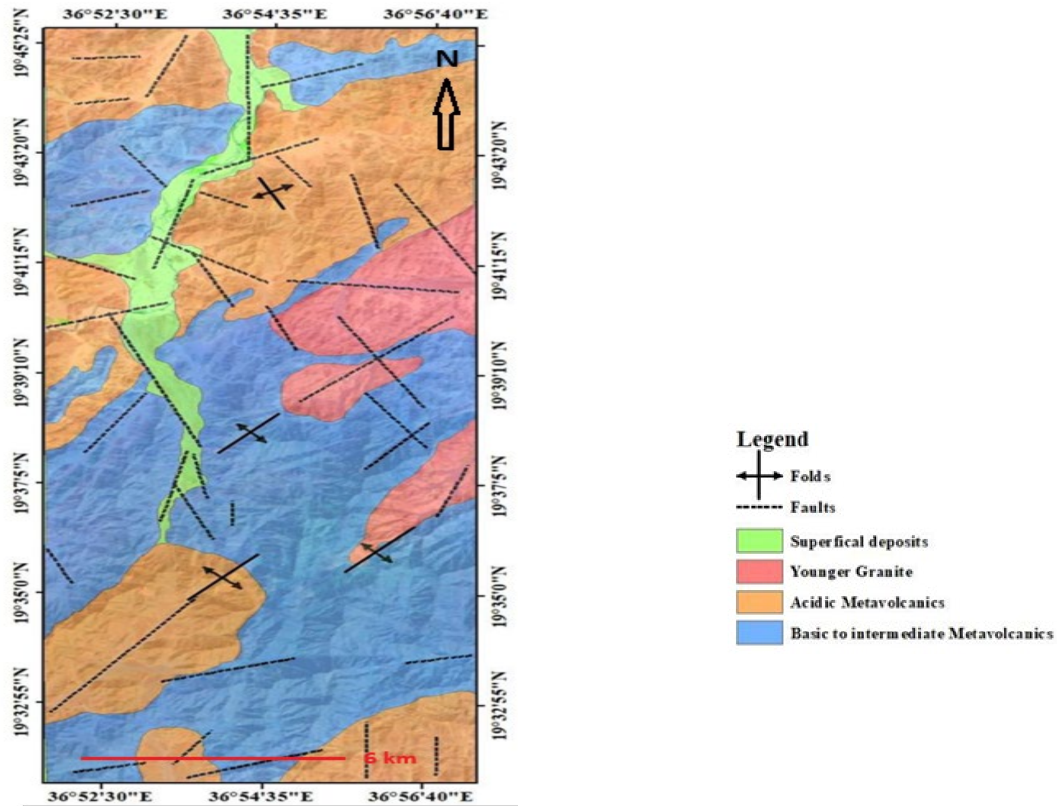

Fig. 2. Regional geological map of the project area

4. SCOPE OF WORK

Within this scope, the study is designed to highlight many important geophysical studies, which could further be integrated with other geological data to use in solving questions concerning locating the potential mineralization zones or other structural setting in term of shape, length, width and depth and to provide targets and leads for future exploration work.

In order to meet the objectives of the site investigation for this exploration, the Satellite Gravity work is suggested:

- Detecting Density Variations: Gold ore deposits often have different densities compared to the surrounding host rocks, creating gravity anomalies (variations in the Earth's gravitational field) that can be detected from space.
- Identifying Subsurface Structures: Satellite gravity data can reveal large-scale geological structures, such as faults and intrusive bodies, which are important controls for Gold mineralization.
- Data Fusion: Satellite gravity data is rarely used in isolation. It is often integrated with other remotely sensed data (e.g., multispectral and hyperspectral imagery) and geological maps to provide a comprehensive understanding of the area.
- Enhancing Geological Mapping: Gravity data helps to improve surface and subsurface geological mapping by providing information on lithological units and structural trends, which are key factors for mineral exploration.

- Interpretation Techniques
  - **Bouguer Anomaly Analysis:** Analyzing Bouguer anomalies (gravity values corrected for topography and depth) can help in isolating both regional and local features of interest, including high-density ore bodies.
  - **First Derivative Analysis:** Analyzing the derivatives of gravity anomalies, such as the first derivative, helps in enhancing features and identifying the edges of high-density structures within the gravity field.
  - 3D Inversion: 3D inversion techniques can be applied to the gravity data to create density models of the subsurface, allowing for a better understanding of the depth and geometry of potential ore bodies.
  - **Analytical Signal (AS):** Locates the edges of gravity sources independent of magnetization direction or data orientation. The amplitude of the analytical signal peaks directly over the causative source edges.
  - **Horizontal Gradient (HG):** Defines the horizontal position of density boundaries. High horizontal gradient values delineate geological contacts and faults.
  - **Euler Deconvolution:** Estimates the depth and type of gravity source using spatial derivatives. Euler Homogeneity Equation as the following:
- Benefits in Gold Exploration
  - Targeting Potential Zones: The integrated approach helps to pinpoint high-potential zones for gold mineralization, guiding subsequent field investigations and reducing costly drilling efforts.
  - Detecting Deep Orebodies: The gravity method is particularly effective at detecting deep, concealed ore bodies that may not be visible with surface surveys alone.

5. METHODOLGY

To achieve the objectives of the study, a combined methods approach was used. It includes RS, GIS based on Satellite Gravity and airborne magnetic. The methodology could be summarized as follows:

- Obtaining general geological information from the regional geological maps of Sudan.
- Compilation of existing geological, and geochemical data, reports, and maps pertaining to this study from BN Energy company.
- Analyzing and processing of satellite gravity and airborne magnetic survey data to generate a structural framework and a depth to basement interpretation for the study area.
- Detection of high potential mineralization zones-based satellite gravity and airborne magnetic survey data.
- Integration of geophysical data to construct a mineralization utility map of the area encompassing different parameters,

5.1. Data and Methods

Gridded Bouguer gravity used. Processing included detrending, residual computation, derivatives, analytical signal, FFT vertical derivative, Euler deconvolution and DBSCAN clustering (Tabel 2).

Key Processing Parameters

Table 2. Euler deconvolution and DBSCAN clustering

Parameter	Value
Structural Index (N)	1
Euler Window Size	5 x 5
DBSCAN eps (std coords)	0.5 (recommended)
DBSCAN min samples	5
FFT vertical derivative	2D FFT on gridded data
CRS	UTM Zone 37N (EPSG:32637)

5.2. Software and Tools Used

Microsoft Excel, Python (NumPy, SciPy, Matplotlib, Scikit-learn), Geosoft, and QGIS

5.3. Satellite Gravity Processing Workflow

5.3.1. Satellite Gravity Enhancement

A suite of filtered grids was generated from the Bouguer gravity field of both surveys to assist interpretation. Wavelength filtering is a means of enhancing features within a certain wavelength range from the full spectrum; for example, low-pass filters provide a long wavelength regional field, whereas high-pass filters produce a shorter wavelength residual field. Figures (3.1) show the Bouguer gravity grid before and after application remove regional gravity. It can be seen that these filters have removed some of the broader, regional anomalies and has accentuated the smaller anomalies seen in the Bouguer grid (Fig. 3.2, 3.3, 3.4, 3.5, and 3.6).

As well as using filters to aid interpretation, the Horizontal Gradient (HG) of the Bouguer gravity field can also be used to highlight the locations of possible faults and body edges (Fig. 3.3). The HG (pink and red areas) mark the locations where the gravity gradients are at their highest, such as would occur over normal faults and other significant density contrasts.

5.3.2. Bouguer Gravity Regional Anomaly

The Free-Air Correction accounts for the decrease of gravity with increasing elevation due to the increased distance from the Earth's center. The correction increases the observed gravity value to what it would be at sea level.

$$\Delta g_{FA} = 0.3086 \times h$$

where:
Δg_{FA} = Free-Air correction (mGal)
h = elevation above sea level (m)

The Bouguer correction removes the gravitational attraction of the rock mass between the observation point and sea level. Typical density: 2.67 g/cm³ for average crustal rocks.

$$\Delta g_B = 0.04192 \times \rho \times h$$

where:
ρ = density of the rocks (g/cm³)
h = station elevation (m)

The CBA represents the corrected gravity after applying latitude, Free-Air, Bouguer, and terrain corrections.

$$g_{CBA} = g_{obs} - \Delta g_{FA} + \Delta g_B + \Delta g_T$$

where:
gobs = observed gravity (mGal)
ΔgT = terrain correction (mGal)

CBA values reflect subsurface density variations caused by geological structures.

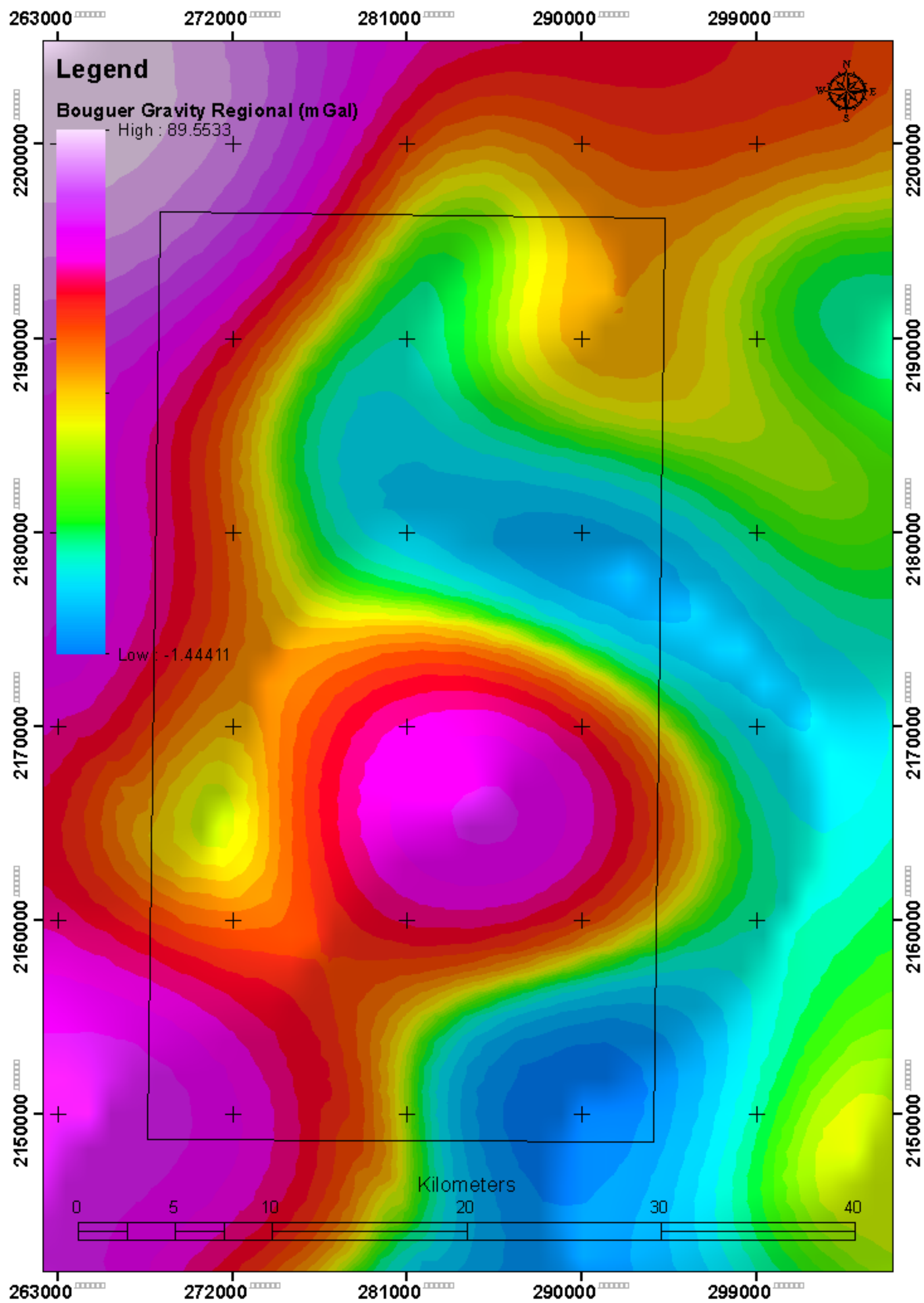

Fig. 3.1. Bouguer Gravity Regional Anomaly map of the project area

5.3.3. Bouguer Gravity Residual Anomaly

To isolate local (residual) gravity anomalies from broad regional trends caused by deep-seated sources.

$$g_{res} = g_{CBA} - g_{reg}$$

where:

g_{reg} = fitted regional surface

g_{res} = residual anomaly used for local structure interpretation.

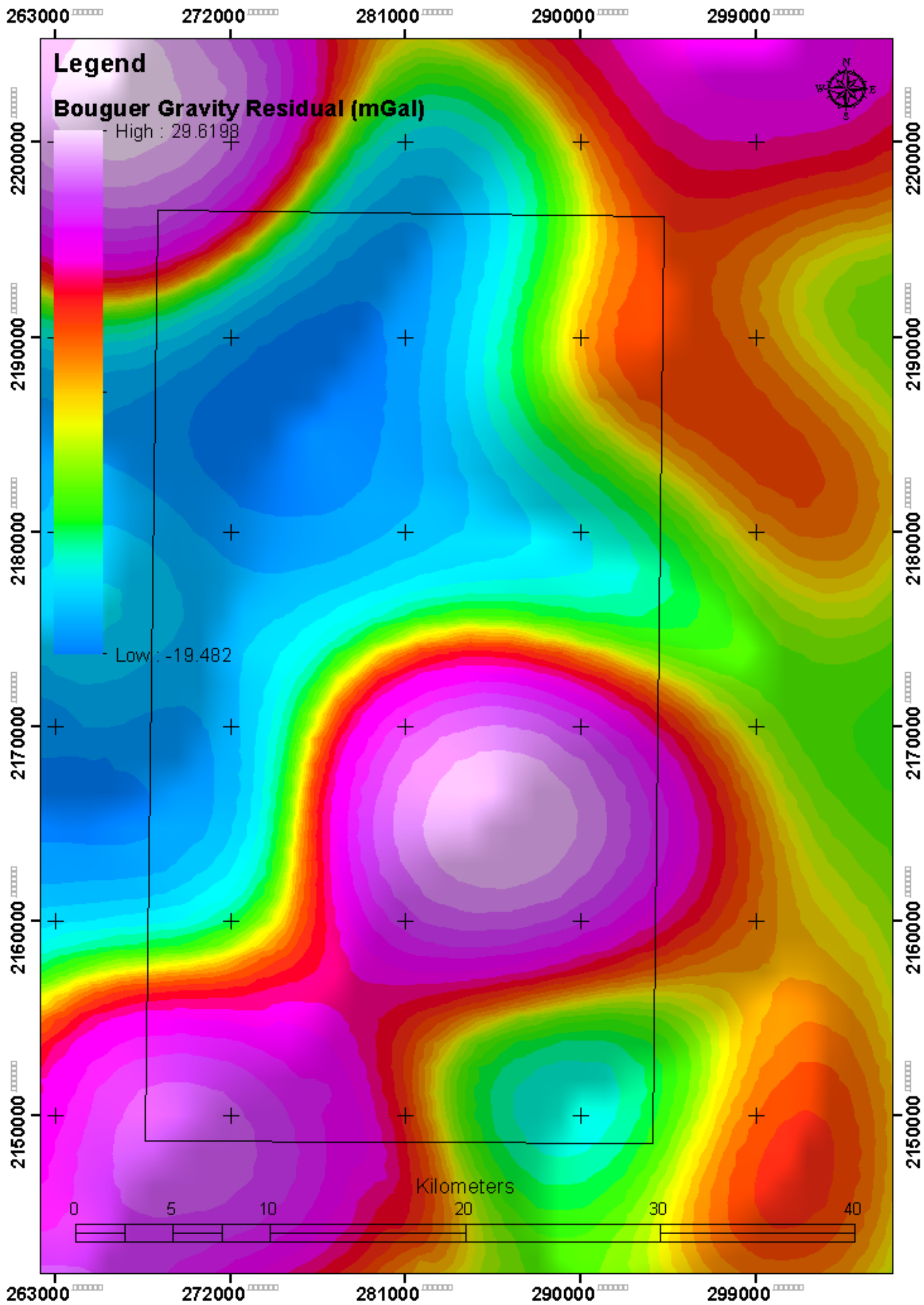

Fig. 3.2. Bouguer Gravity Residual Anomaly map of the project area

5.3.4. Bouguer Gravity First Derivative

Enhances shallow, high-frequency gravity anomalies and suppresses deep, regional effects.

$$\frac{\partial g}{\partial z} \approx \frac{g_{i+1} - g_{i-1}}{2h}$$

Highlights near-surface density contrasts and edges of bodies. The 2VD amplifies noise and should be applied to smoothed data.

$$\frac{\partial^2 g}{\partial z^2} \approx \frac{g_{i+1} - 2g_i + g_{i-1}}{h^2}$$

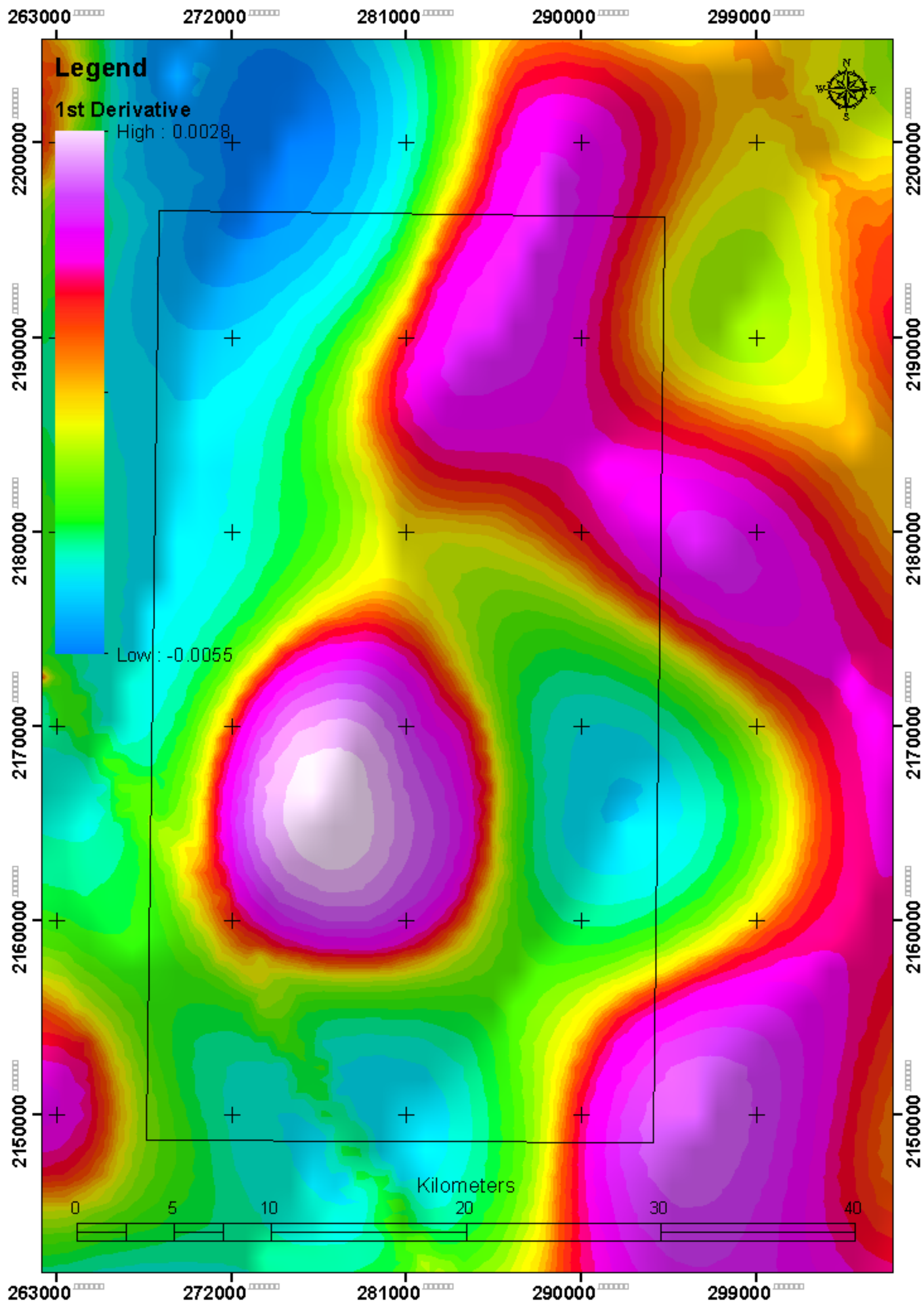

Fig. 3.3. Bouguer Gravity First Derivative map of the project area

5.3.5. Bouguer Gravity Horizontal Gradient

Locates the edges of gravity sources independent of magnetization direction or data orientation. The amplitude of the analytical signal peaks directly over the causative source edges.

$$A(x, y) = \sqrt{\left(\frac{\partial g}{\partial x}\right)^2 + \left(\frac{\partial g}{\partial y}\right)^2 + \left(\frac{\partial g}{\partial z}\right)^2}$$

Defines the horizontal position of density boundaries. High horizontal gradient values delineate geological contacts and faults.

$$HG = \sqrt{\left(\frac{\partial g}{\partial x}\right)^2 + \left(\frac{\partial g}{\partial y}\right)^2}$$

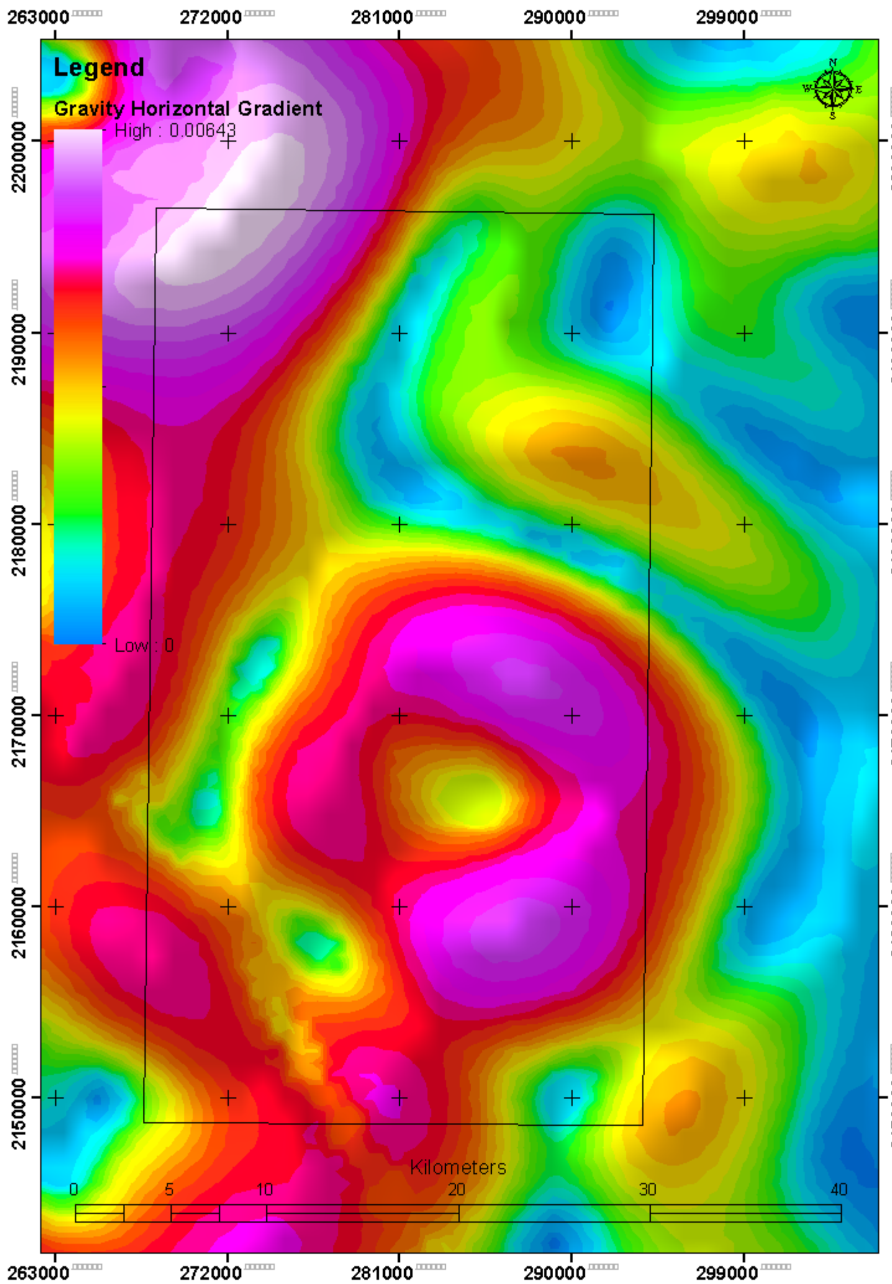

Fig. 3.4. Bouguer Gravity Horizontal Gradient map of the project area

5.3.6. Euler Depth Solutions

Estimates the depth and type of gravity source using spatial derivatives. Euler Homogeneity Equation as the following:

$$(x - x_0)\left(\frac{\partial g}{\partial x}\right) + (y - y_0)\left(\frac{\partial g}{\partial y}\right) + (z - z_0)\left(\frac{\partial g}{\partial z}\right) = N\,(B - g)$$

where:

(x_0, y_0, z_0) = source location; g = measured gravity anomaly; B = regional background field and N = structural index

Common structural indices (N): Contact/Fault: 0, Thin Sheet: 1, Cylinder/Dyke: 2, and Sphere: 3.

5.3.7. Cluster Centroids and Summary

Cluster ID	Centroid X	Centroid Y	Mean Depth	Num.Points	Spread X	Spread Y	Spread Depth
0.00	285434.77	2175858.76	300.82	3072.00	13686.23	21599.03	587.37

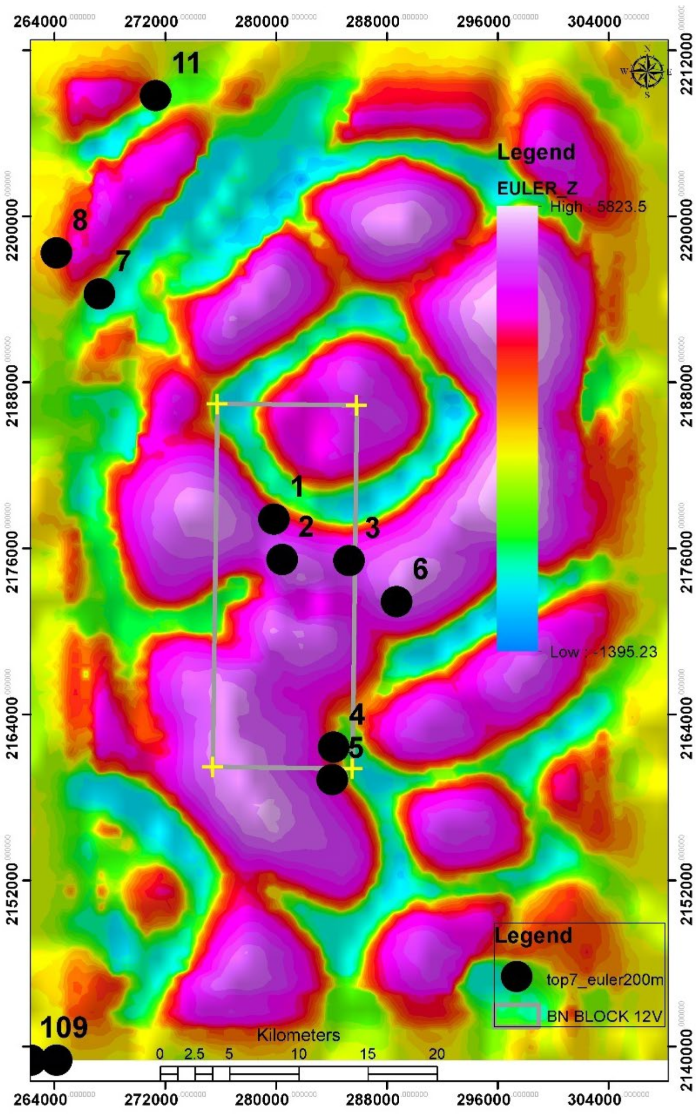

Fig. 3.5. Euler Depth map of the project area superimpose the target points

5.3.8. Euler Deconvolution and Clustering Analysis

Euler deconvolution applied with N=1 and 5x5 windows. Solutions clustered by DBSCAN.

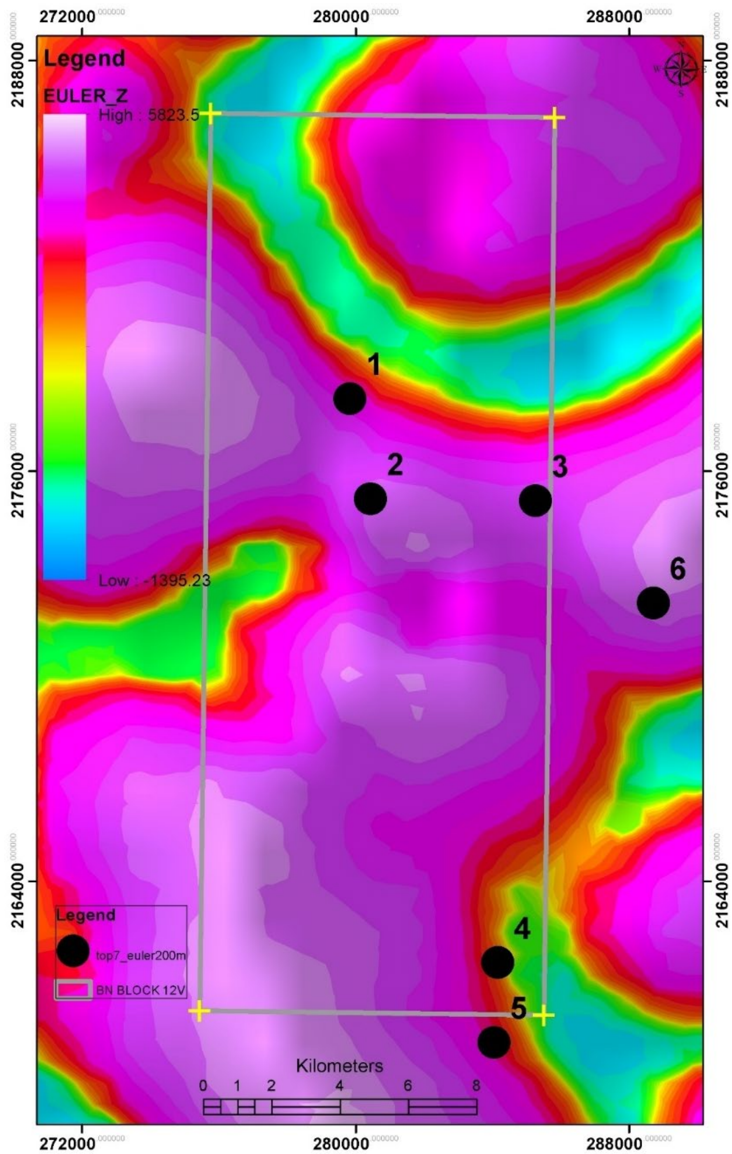

Fig. 3.6. Euler Deconvolution Depth map of the project area

5.4. Magnetic Data Enhancement

AMMP airborne magnetic data for this study were collected covering the satellite gravity area. The Total Magnetic Intensity (TMI) grid for the study area is shown in Figure (3.7). The obvious data enhancement to apply to magnetic data is the Reduction-To-Pole (RTP) transform. The RTP centers magnetic anomalies over their causative sources and produces positive anomalies over magnetic bodies thus helping to simplify the magnetic map. However, RTP transformations are highly unstable and can introduce artefacts when transforming data, which are located close to the magnetic equator (as is the case in the study area). Therefore, the TMI was predominantly used for the interpretation work.

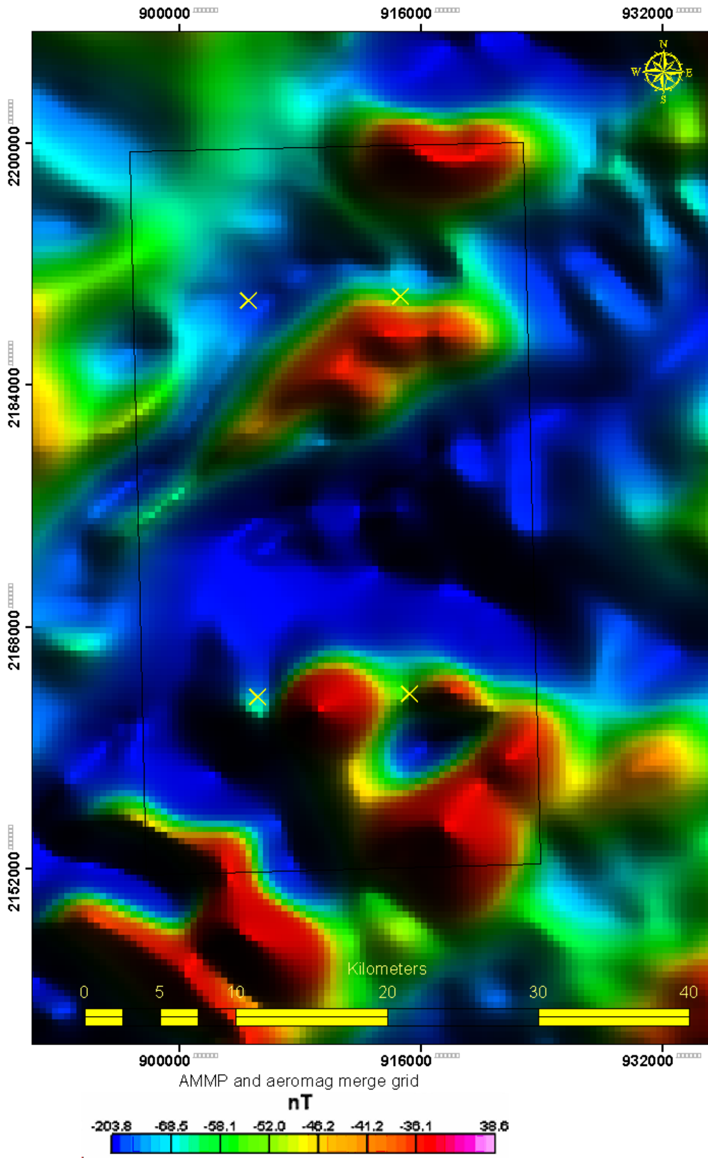

Fig. 3.7. Total Magnetic Intensity (TMI) grid for the project area

5.5. Structure Mapping Results

A number of structure and Precambrian basement features have been identified in the Project areas. Precambrian basement outcrop has been mapped and is based upon the surface geology map but refined according to the observed satellite gravity and AMMP airborne magnetic data. The Precambrian and structure features have been categorised as the following: structure zones areas which display large, negative magnetic responses consistent with the presence of high susceptibility material either within basement. Low Density Basement - sections of upper crust which exhibit lower gravity anomalies than adjacent sections. These gravity lows are not thought to be due to structure but rather due to basement composition variation i.e., the presence of lower density granites or metasediments for example. Magmatic Bodies isolated magmatic features/intrusions which correspond with localised, high amplitude gravity and magnetic anomalies.

Figures (4.1 and 4.2) show the interpretation of Precambrian and structure features for the Project area. The interpretation is overlain upon the Residual Gravity, and the Bouguer Gravity Horizontal Gradient (BG-HG) respectively. It can be seen that a large number of Precambrian and structure features have been interpreted in the study area. A number of structures have been mapped and refined to the centeral part, NE, NW and SW of the Project area. In the east, these features appear to be overprinted with gravity lows trending N-S to NNE-SSW. It is believed, and has been checked in the Eule Depth modelling, that these gravity lows are caused by structural effects.

The NE margin of the Project area appears to be very clearly defined by a major NE-SW trending normal fault which separates the gravity low of the block RS V12 from the much higher gravity response to the NW.

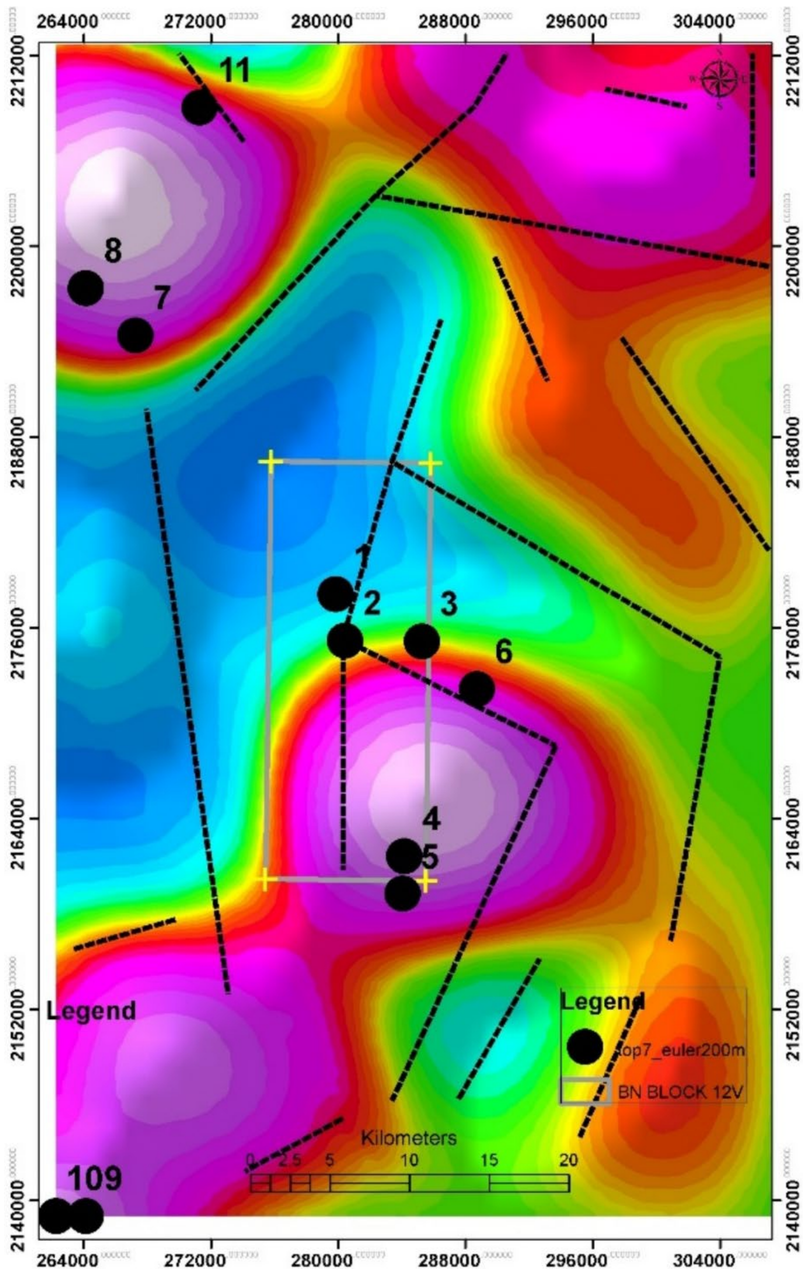

Fig. 4.1. Basement structure features in the project area, overlain upon the Residual Gravity

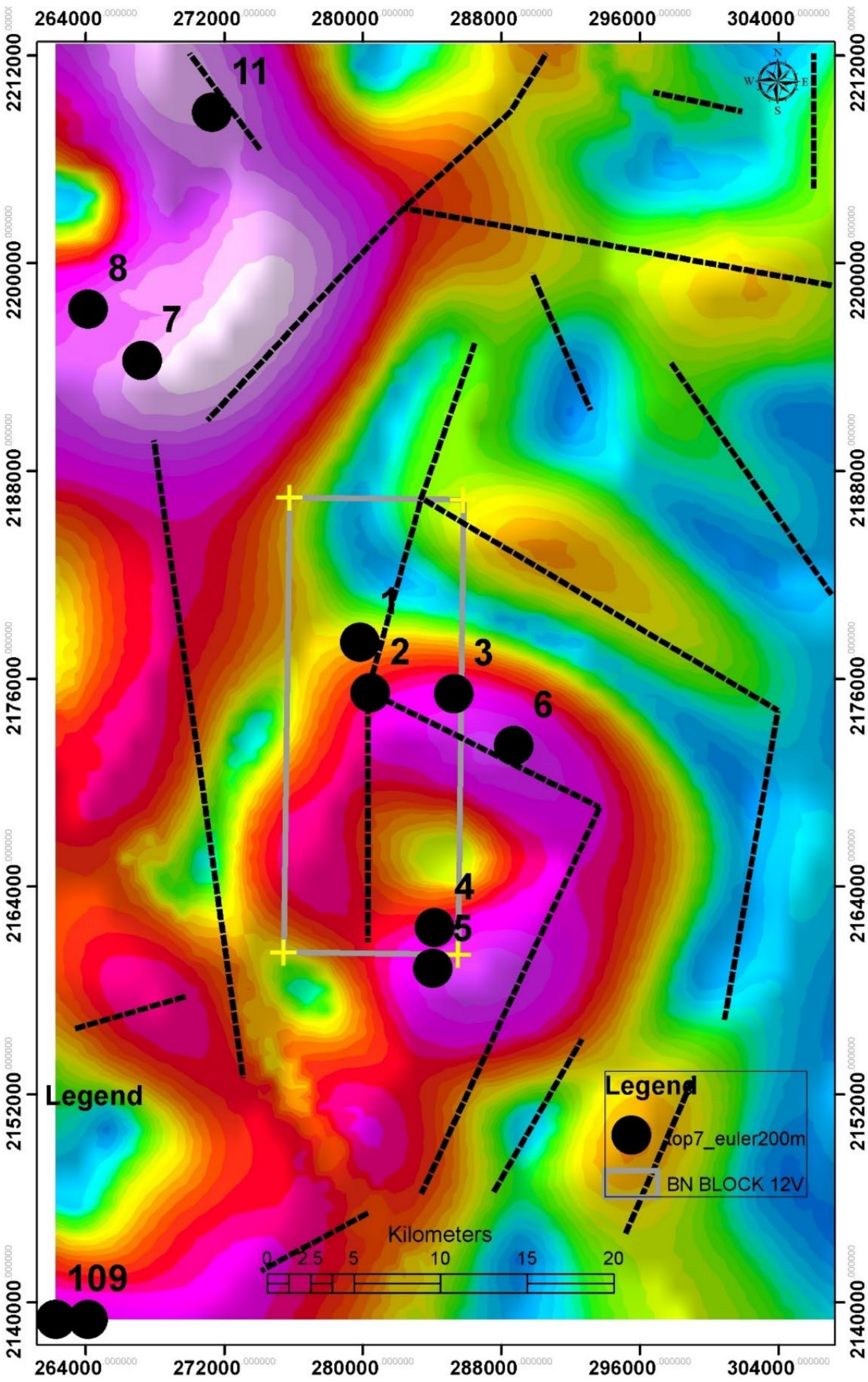

Fig. 4.2. Basement structure features in the project area, overlain upon the Horizontal Gradient

6. MINERALIZATION TARGET ZONES

6.1. Data Available for Target Selection

From satellite gravity workflow as the following:

- **Residual gravity anomaly** – highlights local density contrasts (positive → denser bodies).
- **Analytical signal amplitude (ASA)** – peaks over body edges, good for boundary detection.
- **Vertical derivative (FFT)** – enhances shallow anomalies.
- **Euler deconvolution solutions** – gives estimated source depths.
- **DBSCAN cluster centroids** – show statistically robust source zones.

6.2. Selection Criteria for Mineralization Targets

To select criteria, potential mineralized zones (Table 3), (e.g., **sulfides, and gold-bearing structures**) must be identified by searching for:

Table 3. Selection Criteria for Mineralization Targets

Criterion	Indicator	Interpretation
High Analytical Signal	ASA maxima	Indicates boundary of magneto-dense bodies
Coincident Residual Gravity Highs	Positive anomaly > mean + 1σ	Suggests dense material (e.g., sulfides, Fe)
Shallow Euler Depths	Depth < 1.5 km	Shallow mineralized source
Cluster Density	>5 Euler points per cluster	Stable anomaly cluster
Crossing Structural Trend	Intersection of lineaments	Possible structural trap zone

6.3. Method to Extract in Practice

Using Satellite Gravity dataset, I can:

i. Load the Euler solutions and cluster centroids.
ii. Recreated derivative fields and Analytical Signal from your Regional Gravity (computed horizontal derivatives, analytical signal, residual) as shown in Figure (5.1).
iii. Computed a stable vertical derivative via 2D FFT.
iv. Ran Euler deconvolution (structural index N = 1, window 5×5) and stored per-point solutions.
v. Clustered solutions using DBSCAN (eps = 0.5 on standardized coordinates, min samples = 7) shown in Figure (5.2).
vi. Computed cluster statistics: mean depth, mean residual gravity, mean analytical signal, count, std.
vii. Calculated an MPI for each cluster:
viii. Rank clusters by a "Mineralization Potential Index (MPI)" such as:

$$\mathrm{MPI} = \frac{\mathrm{A}_{\mathrm{ASA}} \times \mathrm{A}_{\mathrm{Residual}}}{\mathrm{D}_{\mathrm{Euler}}}$$

(Where A = amplitude, D = depth).

ix. The top 2–3 clusters with high ASA/residual and shallow Euler depths will be recommended as mineralization zones.

x. Output a map and table showing ranked potential targets.

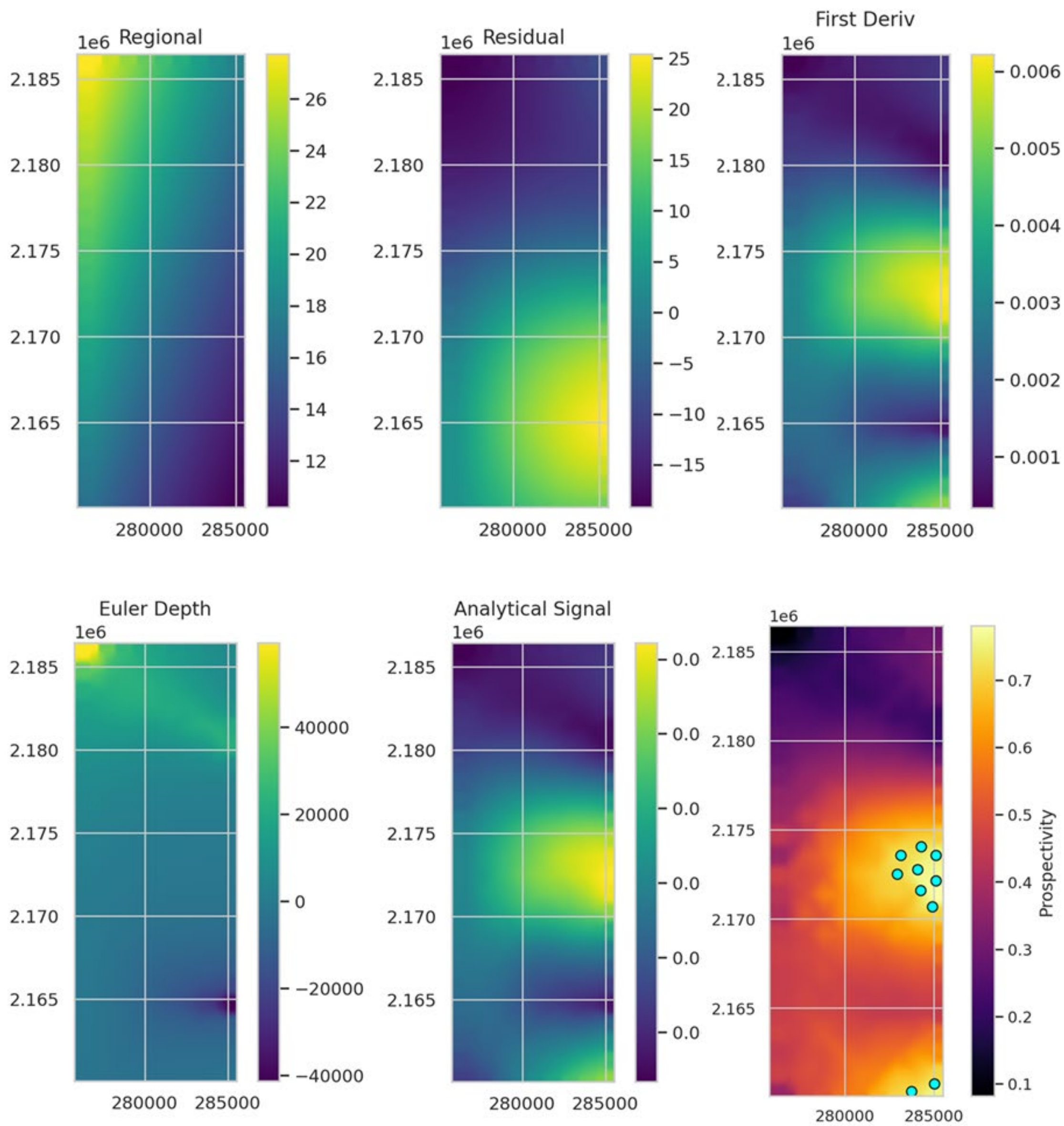

Fig. 5.1. Satellite Gravity Data model

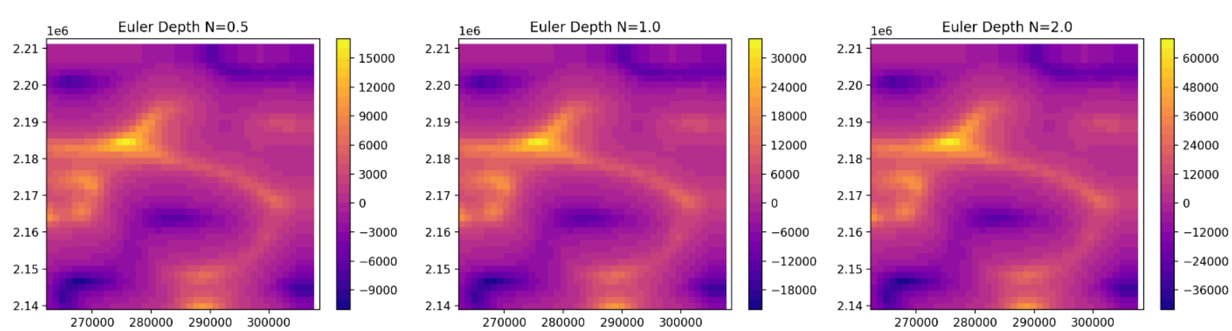

Fig. 5.2. Euler Deconvolution applied with N=0.5, 1 and 2.0 Euler Depth

6.4. Output Receive

- ✓ Table: Cluster ID, mean Euler depth, residual anomaly, analytical signal amplitude, MPI score
- ✓ Map: Cluster centroids color-coded by MPI (red = most prospective)

6.5. Exploration targets

Thirty-three exploration targets have been identified within Block RS 12V (4 gold target located inside the block and 7 outside) on the basis of the results of the Satellite Gravity and airborne AMMP Magnetic Data interpretation as shown in Table (4). These targets are based on a number of criteria including:

i.	Available Data
ii.	positive Residual gravity anomaly denser bodies
iii.	Analytical signal amplitude (ASA) – peaks over body edges, good for boundary detection
iv.	Vertical derivative (FFT) – enhances shallow anomalies.
v.	Euler deconvolution solutions – gives estimated source depths.
vi.	DBSCAN cluster centroids – show statistically robust source zones.

Table 4. Mineralization Target

East (X)	North (Y)	Euler Depth	Residual	FVD	Analytical	Target # Rank
279830.66	2178110.53	-1852.49	13.19	0.006490	0.007119	1
280427.00	2175184.00	-1679.08	12.24	0.006384	0.007290	2
285259.92	2175126.02	-2806.73	17.94	0.003154	0.006384	3
284156.60	2161626.96	-1464.38	10.81	0.005800	0.007386	4
284044.86	2159282.94	-2450.90	12.75	0.005229	0.005229	5
288709.18	2172134.23	-1151.17	6.76	0.005816	0.005816	6
267253.33	2194376.83	-1410.29	8.71	0.006283	0.006283	7
264143.79	2197342.51	-3301.13	17.89	0.005448	0.005448	8
264143.79	2139017.46	-5835.99	18.26	0.003162	0.003162	9
262278.07	2139017.46	-4924.65	20.75	0.004211	0.004211	10
271295.74	2208710.95	-1290.95	8.14	0.006449	0.006449	11

The target areas have been assigned a priority ranking of 1 to 11. The most favorable targets in the project area are Priority 1, 2, 3 and 4 as shown in Table (4).

The mineralization targets with structure and gravity anomalies are shown on Figure (6).

The main characteristics of the target areas are presented in the Figure (6).

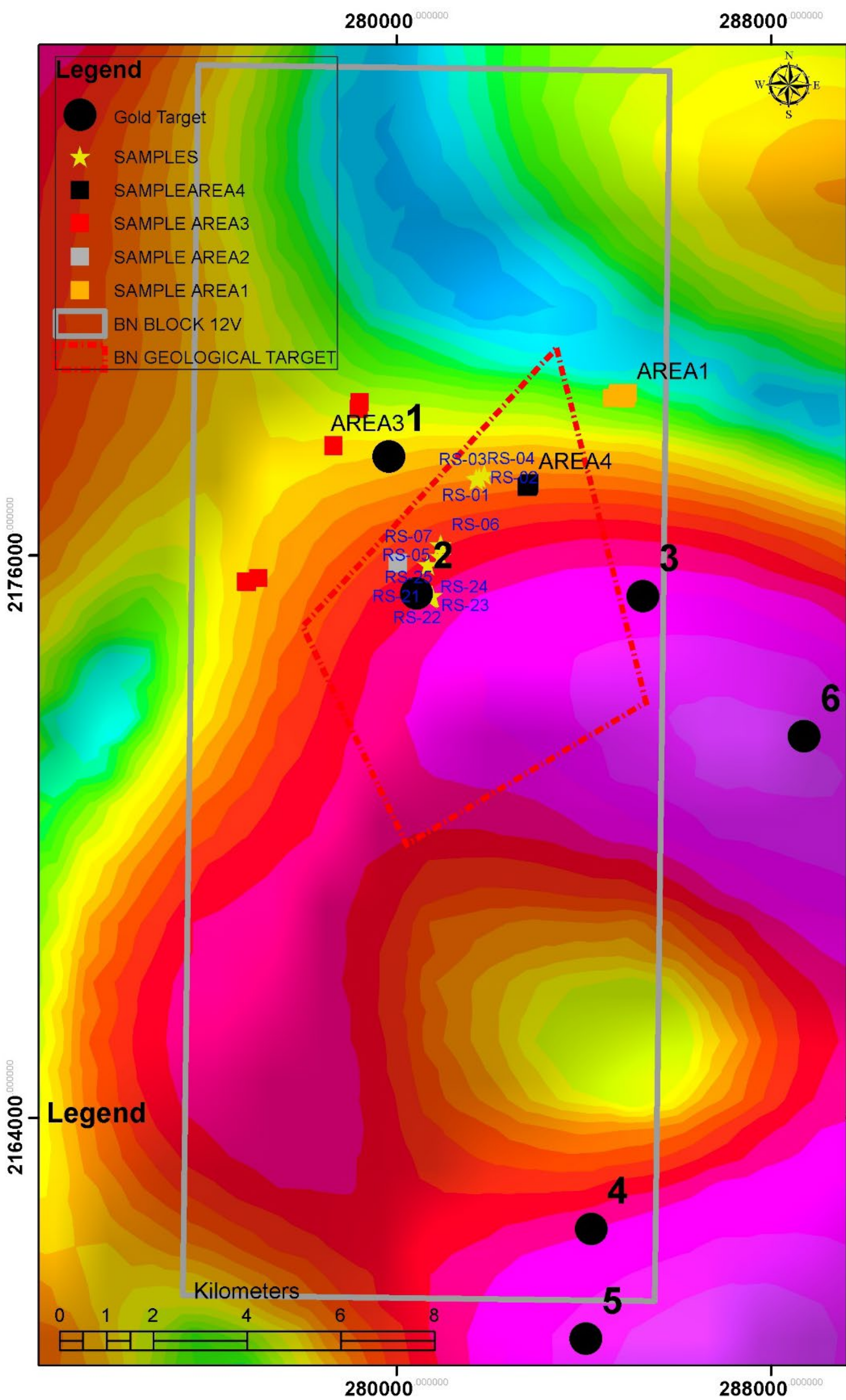

Fig. 6a. The exploration targets overlain upon the Residual Gravity Anomaly, illustrate BN Block 12V, BN gold target area and location of geochemical samples

7. RECOMMENDATION

- MPI is a heuristic index combining amplitude (signal strength) and depth; it **does not** guarantee mineralization, it prioritizes targets that are strong (ASA and residual) and relatively shallow.
- The sample result shows one cluster (ID 0) with MPI ≈ 1.85×10^{-8} (this is small because anomalies and depths are small; ranking is relative).
- I recommend focusing on the **top 1–4 ranked clusters** for follow-up:
  - Validate with geological maps / lineaments.
  - Conduct ground magnetic surveys to refine depth and geometry.
  - Conduct geo-electrical surveys to refine depth and geometry.
  - Model A targets emphasize shallower Euler solutions (200 m vs 300 m). Model B clusters top anomalous pixels and captures coherent multivariate anomaly zones. Use both sets jointly for prioritization

8. References

Telford, W.M., Geldart, L.P., Sheriff, R.E. (1990). Applied Geophysics, 2nd ed.
Nabighian, M.N. (1972). Analytical Signal of Two-dimensional Magnetic Bodies.
Reid, A.B. et al. (1990). Magnetic Interpretation Using Euler Deconvolution.
Blakely, R.J., 1996. Potential Theory in Gravity and Magnetic Applications. Cambridge University Press.